

## Strange-Meson Spectroscopy at COMPASS

S. Wallner\* for the COMPASS collaboration

*Physics Department, Technical University of Munich,  
Garching, 85748, Germany*

*\*E-mail: stefan.wallner@tum.de*

COMPASS is a multi-purpose fixed-target experiment at CERN aimed at studying the structure and spectrum of hadrons. It has collected the so far world's largest data set on diffractive production of the  $K^- \pi^- \pi^+$  decay, which in principle gives access to all kaon states. We performed an elaborate partial-wave analysis, using model-selection techniques to select the wave set based on a large systematically constructed pool of allowed partial waves. The partial-wave decomposition reveals signals in the mass region of well-known states, such as  $K_1(1270)$  and  $K_1(1400)$ . In addition, we observe potential signals from excited states, such as  $K_1(1650)$ .

*Keywords:* COMPASS; Strange Mesons; Spectroscopy; Proceedings; HADRON 2019; XVIII International Conference on Hadron Spectroscopy and Structure

### 1. Meson Spectroscopy at COMPASS

COMPASS is a fixed-target multi-purpose experiment located at CERN. So far, COMPASS has studied mainly isovector resonances of the  $a_J$  and  $\pi_J$  families with high precision, using the dominant  $\pi^-$  component of the 190 GeV/c negative hadron beam.<sup>1,2</sup> In this analysis, we study the strange-meson spectrum up to masses of 3 GeV/ $c^2$  using the approximately 2.4%  $K^-$  fraction of the beam in diffractive scattering off a liquid-hydrogen target. Our flagship channel is the production of  $K^- \pi^- \pi^+$ , which in principle gives access to all kaon states, i.e.  $K_J$  and  $K_J^*$  mesons.<sup>a</sup> COMPASS acquired the so far world's largest data set of about 720 000 exclusive events for this channel.

### 2. Kinematic Distributions

Figure 1a shows the invariant mass spectrum of the  $K^- \pi^- \pi^+$  final state. It exhibits structures in the  $m_{K\pi\pi}$  region of well-known resonances, e.g.

<sup>a</sup>Except for  $J^P = 0^+$  states.

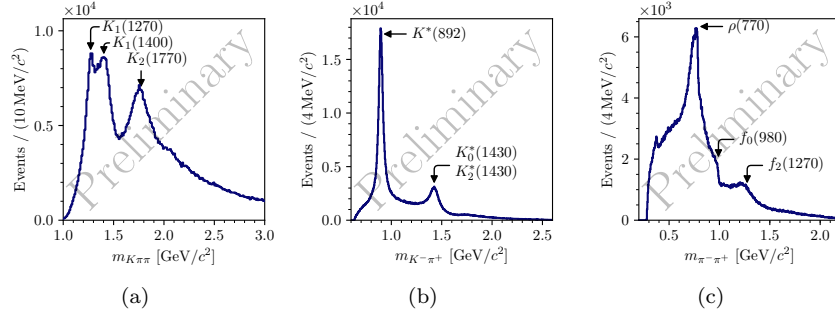


Fig. 1. Invariant mass distribution of the  $K^- \pi^- \pi^+$  system (a) and of the  $K^- \pi^+$  (b) and  $\pi^- \pi^+$  (c) sub-systems. The distributions are not corrected for acceptance effects, which are significant in certain regions of the phase space.

$K_1(1270)$  or  $K_1(1400)$ , which sit on top of a broad distribution. The invariant mass distributions of the  $K^- \pi^+$  and  $\pi^- \pi^+$  sub-systems are dominated by well-known two-body resonances as indicated by the labels in Figs. 1b and 1c.<sup>b</sup> This dominance of two-body resonances justifies the application of the isobar model in the partial-wave decomposition, which is discussed in the following section.

### 3. Analysis Method: Partial-Wave Decomposition

We employ the method of partial-wave analysis to decompose the data into contributions from various partial waves (see Ref. 1 for details). To this end, we construct a model for the intensity distribution  $\mathcal{I}(\tau)$  of the  $K^- \pi^- \pi^+$  final state in terms of the five phase-space variables that are represented by  $\tau$ . Using the isobar approach,  $\mathcal{I}(\tau)$  is modeled as a coherent sum of partial-wave amplitudes

$$\mathcal{I}(\tau; m_{K\pi\pi}, t') = \left| \sum_a^{\text{waves}} \mathcal{T}_a(m_{K\pi\pi}, t') \psi_a(\tau; m_{K\pi\pi}) \right|^2. \quad (1)$$

These partial waves are represented by  $a = J^P M^\epsilon \zeta b L$  and are defined by the quantum numbers of the  $K^- \pi^- \pi^+$  system ( $J^P M^\epsilon$ ),<sup>c</sup> the intermediate

<sup>b</sup>The small spike at about  $0.4 \text{ GeV}/c^2$  in the  $m_{\pi^- \pi^+}$  system originates from  $\phi \rightarrow K^- K^+$  decays from a small contamination of the  $K^- \pi^- \pi^+$  data sample by  $K^- K^- K^+$ , where the kaons are misidentified as pions.

<sup>c</sup>Here,  $J$  is the spin of the  $K^- \pi^- \pi^+$  state and  $P$  its parity. The spin projection of  $J$  along the beam axis is given by  $M^\epsilon$ .

two-body resonance  $\zeta^d$ , and the orbital angular momentum  $L$  between the bachelor particle  $b$  and the isobar. Within the isobar model, the decay amplitudes  $\psi_a$  can be calculated. This allows us to extract the partial-wave amplitudes  $\mathcal{T}_a$ , which determine strength and phase of each wave from the data by an unbinned maximum-likelihood fit.

In order to extract the dependence of the partial-wave amplitudes on the invariant mass  $m_{K\pi\pi}$  of the  $K^-\pi^-\pi^+$  system and on the squared four-momentum transfer  $t'$  between the beam particle and the target proton, the maximum-likelihood fit is performed independently in 75 narrow bins of  $m_{K\pi\pi}$  and 4 bins of  $t'$  in the analyzed kinematic range of  $1.0 < m_{K\pi\pi} < 3.0 \text{ GeV}/c^2$  and  $0.1 < t' < 1.0 (\text{GeV}/c)^2$ .

In order to construct the wave set, i.e. the partial waves that enter the sum in Eq. (1), we apply model-selection techniques. We systematically construct a large set of possible partial waves, called wave pool. We restrict ourselves to  $J \leq 7$ ,  $L \leq 7$ , positive naturality of the exchange particle, and twelve isobars: two  $K\pi$   $S$ -wave amplitudes,  $K^*(892)$ ,  $K^*(1680)$ ,  $K_2^*(1430)$ ,  $K_3^*(1780)$ , a broad  $\pi\pi$   $S$ -wave amplitude,  $f_0(980)$ ,  $f_0(1500)$ ,  $\rho(770)$ ,  $f_2(1270)$ , and  $\rho_3(1690)$ .<sup>e</sup> This results in a wave pool of 596 allowed waves. In order to select the wave set, we fit the wave pool to the data applying regularization techniques to suppress insignificant waves (see Ref. 3 for details). This results in an individual wave set for each  $(m_{K\pi\pi}, t')$  cell, which we fit again to the data without regularization terms.

## 4. Selected Results of the Partial-Wave Decomposition

### 4.1. $J^P = 1^+$ Waves

The  $1^+0^+K^*(892)\pi S$  wave is the most dominant one in our data. It accounts for about 30% of the total intensity. Fig. 2a shows the  $t'$ -summed intensity spectrum, i.e. the intensity spectrum incoherently summed over the four  $t'$  bins, of the  $1^+0^+K^*(892)\pi S$  wave. Two peaks are visible in the mass regions of the  $K_1(1270)$  and the  $K_1(1400)$  in agreement with previous observations.<sup>4</sup> Systematic studies of our analysis revealed, that the low-mass region, indicated by the gray area in Fig. 2a, of this wave and some other waves not discussed here is affected by systematic effects. These effects arise mainly from the limited kinematic range of the COMPASS final-

<sup>d</sup>We consider isobar resonances in the  $K^-\pi^+$  or  $\pi^-\pi^+$  sub-system.

<sup>e</sup>We use relativistic Breit-Wigner amplitudes for all isobar line shapes, except for the  $S$ -wave isobars, where we employ  $K$ -matrix parameterizations.

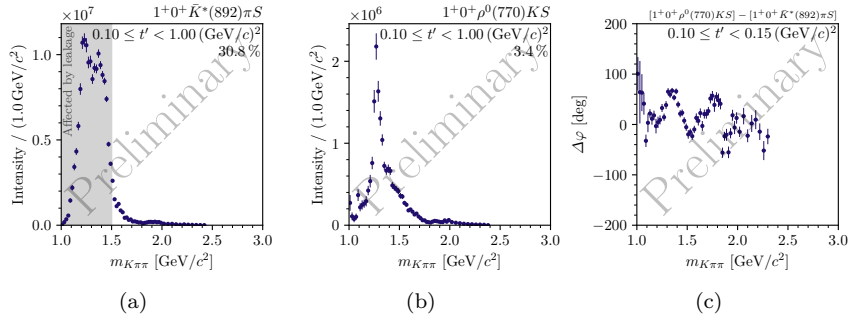


Fig. 2.  $t'$ -summed intensity distributions of the  $J^P M^z = 1^+0^+$  partial waves in the  $K^*(892)\pi S$  (a) and the  $\rho(770)KS$  (b) decay. (c) shows the relative phase between these two partial waves in the lowest  $t'$  bin.

state particle identification and are under further study. Therefore, the low-mass region of the  $1^+0^+K^*(892)\pi S$  wave should be considered only on a qualitative level.

The intensity spectrum of the  $1^+0^+\rho(770)KS$  wave, shown in Fig. 2b, exhibits only one dominant peak in the mass region of the lower-lying  $K_1(1270)$ . We observe a bump in its high-mass shoulder at about  $1.6\text{ GeV}/c^2$ . The PDG<sup>5</sup> lists the  $K_1(1650)$  resonance in this mass region, which needs further clarification.

Figure 2c shows the relative phase between the  $1^+0^+\rho(770)KS$  and the  $1^+0^+K^*(892)\pi S$  wave. It exhibits rich structures. First, the phase rises in the  $K_1(1270)$  mass region, which can be explained by the dominance of the  $K_1(1270)$  in the  $\rho(770)KS$  decay.<sup>f</sup> Then, the relative phase drops in the mass region of the  $K_1(1400)$ . This can be explained by the strong contribution of the  $K_1(1400)$  to the  $K^*(892)\pi S$  decay, which enters with a minus sign in the relative phase. Finally, the relative phase rises again at about  $1.7\text{ GeV}/c^2$ . This could be a potential indication of the  $K_1(1650)$  resonance in the  $\rho(770)KS$  decay.

#### 4.2. $J^P = 2^-$ Waves

The  $2^-$  waves show a large variety of different structures in various decay modes. The most dominant signal is in the  $2^-0^+K_2^*(1430)\pi S$  wave shown

<sup>f</sup>The phase motion produced by the  $K_1(1270)$  resonance in the  $K^*(892)\pi S$  decay is potentially smeared out by the low-mass tail of the  $K_1(1400)$ .

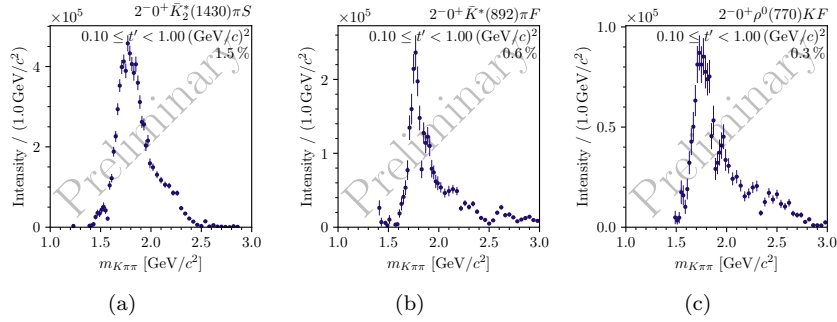


Fig. 3.  $t'$ -summed intensity distributions of the  $J^P M^z = 2^{-0^+}$  partial waves in the  $K_2^*(1430)\pi S$  (a),  $K^*(892)\pi F$  (b), and the  $\rho(770)KF$  (c) decay.

in Fig. 3a, which accounts for about 1.5% of the total intensity. It exhibits a broad peak at about  $1.8 \text{ GeV}/c^2$  with a bump in its high-mass shoulder. The PDG<sup>5</sup> lists the established resonances  $K_2(1770)$  and  $K_2(1820)$  in the mass region of the peak and the  $K_2(2250)$ , which needs further confirmation, in the mass region of the high-mass bump.

The  $2^{-0^+}K^*(892)\pi F$  wave shows a narrow peak at about  $1.8 \text{ GeV}/c^2$  with a bump in its high-mass shoulder. Also the  $2^{-0^+}\rho(770)KF$  wave exhibits a peak at about  $1.8 \text{ GeV}/c^2$ . Its high-mass shoulder contains more complicated structures, which potentially also contain the  $K_2(2250)$  resonance. To clarify the nature of the observed signals and to extract their parameters, i.e. masses and widths, a resonance-model fit similar to Ref. 2 will be the next major step in this analysis.

## References

1. C. Adolph *et al.*, Resonance production and  $\pi\pi$   $S$ -wave in  $\pi^- + p \rightarrow \pi^- \pi^- \pi^+ + p_{\text{recoil}}$  at  $190 \text{ GeV}/c$ , *Physical Review D* **95**, p. 032004 (2017).
2. M. Aghasyan *et al.*, Light isovector resonances in  $\pi^- p \rightarrow \pi^- \pi^- \pi^+ p$  at  $190 \text{ GeV}/c$ , *Physical Review D* **98**, p. 092003 (2018).
3. F. Kaspar *et al.*, Wave-selection techniques for partial-wave analysis in light-meson spectroscopy, within these proceedings.
4. C. Daum *et al.*, Diffractive production of strange mesons at  $63 \text{ GeV}$ , *Nuclear Physics B* **187**, 1 (1981).
5. M. Tanabashi *et al.*, Review of Particle Physics, *Physical Review D* **98**, p. 030001 (2018).